Vol 15 No 12, December 2006
1009-1963/2006/15(12)/2963-07
Chinese Physics
© 2006 Chin. Phys. Soc.
and IOP Publishing Ltd

Temperature-related performance of Yb^{3+}:YAG disc lasers and optimum design for diamond cooling

Cao Ding-Xiang(曹丁象)[a)b)†], Yu Hai-Wu(於海武)[b)], Zheng Wan-Guo(郑万国)[b)],
He Shao-Bo(贺少勃)[b)], and Wang Xiao-Feng(王晓峰)[a)]

[a)] *National University of Defence Technology, Changsha* 410073, *China*

[b)] *Research Center of Laser Fusion, CAEP, Mianyang* 621900, *China*

(Received 3 March 2006; revised manuscript received 28 May 2006)

In this paper the temperature-related performances of the Yb^{3+}:YAG disc laser has been investigated based on quasi-three level rate equation model. A compact diamond window cooling scheme also has been demonstrated. In this cooling scheme, laser disc is placed between two thin discs of single crystal synthetic diamond, the heat transfer from Yb^{3+}:YAG to the diamond, in the direction of the optical axis, and then rapidly conducted radically outward through the diamond to the cooling water at the circumference of the diamond/Yb^{3+}:YAG assembly. Simulation results show that increasing the thickness of the diamond and the overlap-length (between diamond and water) decreases the disc temperature. Therefore a 0.3–0.5 mm thick diamond window with the overlap-length of 1.5–2.0 mm will provide acceptable cost effective cooling, e.g., with a pump intensity of 15 kW/cm^2 and repetitive rate of 10 Hz, to keep the maximum temperature of the lasing disc below a reasonable value (310K), the heat exchange coefficient of water should be about 3000 W/m^{2}K.

Keywords: Yb^{3+}:YAG, diamond, thermal management, temperature effect, diode-pumped
PACC: 4255R, 4260D

1. Introduction

With improvement of high power laser diodes, the quasi-three level solid state laser medium Yb^{3+}:YAG has attracted a worldwide interest because of its several advantages.[1−3] Firstly, it has a very low pump defect. For example, the Yb^{3+}:YAG results in a factor of 3 less heat generation than Nd^{3+}:YAG. Secondly, the Yb^{3+}:YAG has an upper state lifetime about 1 ms, which is suitable for laser diode pumping. Thirdly, the Yb^{3+}:YAG has a broad-band of absorption about 18 nm (FWHM), and thus the cooling of laser diodes does not need to be controlled accurately, which is important for high power diode pump solid state laser. Finally, Yb^{3+} has simple electronic structure (only two levels $^2F_{5/2}$–$^2F_{7/2}$) which avoids the excited states absorption, up conversion and concentration quenching. Additionally, because the atomic diameter of Yb^{3+} ion (0.0985 nm) approaches that of Y^{3+} (0.1019 nm) ion, YAG can be easily doped at a very high concentration level. However, the performance of Yb^{3+}:YAG laser is impacted remarkably by the temperature.[4−6] The Yb^{3+}:YAG laser has a high pump saturation intensity (∼28 kW/cm^2) which is needed to improve the optical efficiency and thus results in a high heat power density, especially in high repetition rate operation. If the heat is not removed efficiently, the temperature of the lasing medium rises, thereby degrading the efficiency of the lasing action[7−11].

For a quasi-three-level gain medium the product of doping concentration and thickness is constant for fixed pumping condition. Taking into account the cooling effect, we need a thin medium to obtain both high pump intensity and quick cooling, e.g., thin disc configuration, a hundreds μm medium is mounted in a copper sink, but that is the quasi-continuous wave laser or power laser. For the energy laser a thicker medium is needed to obtain high pump energy, e.g., the thickness is respectively 1.4 mm and 1.6 mm for the oscillator and amplifier of LUCIA, a 100J/10 Hz/10 ns diode-pumping solid-state laser facility.[5] But the experiments show that rear face water cooling alone could not cool the medium efficiently.[5] In this paper, we employ a chemical vapour deposition (CVD) diamond window cooling scheme. The lasing disc is pumped through a transparent diamond window, whose excellent cooling property is utilized to efficiently remove the heat

†E-mail: caodingxiang02@yahoo.com.cn

from the pumped region.

2. Theoretical investigation of temperature dependence on performance of Yb^{3+}:YAG lasers

The pumping and energy extraction dynamics of quasi-three-level laser ions of Yb^{3+} has been given in detail by Bourdet.[6] The population densities participating in the absorption and the amplification are as follows:

$$\Delta N_{\rm p}=f_{{\rm L}i}N_{\rm L}-f_{{\rm U}j}N_{\rm U}=N_{\rm Yb}(f_{{\rm L}i}+f_{{\rm U}j})(f_{\rm p}-X_{\rm U}),$$
$$\Delta N_{\rm l}=f_{{\rm U}n}N_{\rm U}-f_{{\rm L}m}N_{\rm L}=N_{\rm Yb}(f_{{\rm L}m}+f_{{\rm U}n})(X_{\rm U}-f_{\rm l}), \quad (1)$$

where $X_{\rm U}=N_{\rm U}/N_{\rm Yb}$, and $f_{\rm p}=f_{{\rm L}i}/(f_{{\rm L}i}+f_{{\rm U}j})$, $f_{\rm l}=f_{{\rm L}m}/(f_{{\rm L}m}+f_{{\rm U}n})$, $N_{\rm Yb}$ is the total doping population density, $N_{\rm U}$ and $N_{\rm L}$ are the population densities of upper and lower energy levels, $f_{{\rm L}i}$, $f_{{\rm L}m}$, $f_{{\rm U}j}$ and $f_{{\rm U}n}$ are the Boltzmann occupation factors of the Stark levels. The two characteristic parameters of $f_{\rm p}$ and $f_{\rm l}$ represent the pumping and lasing performances respectively. In this paper, we will take into account the temperature dependence of these parameters, i.e., $f_{\rm p}(T)$ and $f_{\rm l}(T)$.

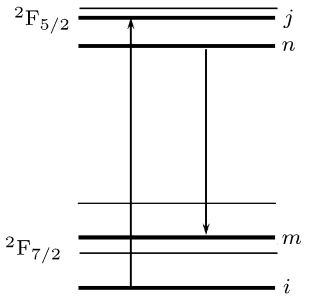


Fig.1. Energy level diagram for Yb^{3+}:YAG.

Then the Boltzmann occupation factors of the levels involved in the transition are expressed as

$$f_{{\rm L}i}=\frac{d_{{\rm L}i}\cdot\exp(-E_{{\rm L}i}/kT)}{Z_{\rm L}},$$
$$f_{{\rm U}j}=\frac{d_{{\rm U}j}\cdot\exp(-E_{{\rm U}j}/kT)}{Z_{\rm U}\cdot\exp(-E_{\rm ZL}/kT)}, \quad (2)$$

where $E_{{\rm L}i}$, $E_{{\rm U}j}$ are the energies of the Stark levels of the lower and upper states, respectively, $Z_{\rm L}$, $Z_{\rm U}$ are lower and upper manifold partition functions, $E_{\rm ZL}$ is the 'zero line' which corresponds to the energy separating the lowest levels of the lower and upper states. $Z_{\rm L}$, $Z_{\rm U}$ are given by

$$Z_{\rm U}=\exp(E_{\rm ZL}/kT)\cdot\sum_j d_{{\rm U}j}\cdot\exp(-E_{{\rm U}j}/kT),$$
$$Z_{\rm L}=\sum_i d_{{\rm L}i}\cdot\exp(-E_{{\rm L}i}/kT). \quad (3)$$

Using these notations, we can express the rate equation for the upper laser level as

$$\frac{{\rm d}N_{\rm U}}{{\rm d}t}=\sigma_{\rm p}c\Phi_{\rm p}\Delta N_{\rm p}-\frac{N_{\rm U}}{\tau_{\rm U}}-\sigma_{\rm l}c\Phi_{\rm l}\Delta N_{\rm l}. \quad (4)$$

By use of $X_{\rm U}=N_{\rm U}/N_{\rm Yb}$, Eq (4) can be written as

$$\frac{{\rm d}X_{\rm U}}{{\rm d}t}=\sigma_{\rm p}c\Phi_{\rm p}(f_{{\rm L}i}+f_{{\rm U}j})(f_{\rm p}-X_{\rm U})-\frac{X_{\rm U}}{\tau_{\rm U}}-\sigma_{\rm l}c\Phi_{\rm l}(f_{{\rm L}m}+f_{{\rm U}n})(X_{\rm U}-f_{\rm l}), \quad (5)$$

where $\tau_{\rm U}$ is the excited state lifetime, c is the velocity of light, $\sigma_{\rm p},\sigma_{\rm l}$ are the absorption and emission cross section respectively, $\Phi_{\rm p}$, $\Phi_{\rm l}$ are the photon density for the pump and the laser wave respectively. Expressing Eq.(5) in terms of pump and laser intensity waves ($\Phi_i=T^{\rm k}/ch\nu_{\rm k}$), we obtain a simple relation connecting $X_{\rm U}$ to the pump and laser intensities normalized to their saturation intensities ($I^{\rm k}/I_{\rm ks}$, where $I_{\rm ls}=h\nu_{\rm l}/(f_{{\rm L}m}+f_{{\rm U}n})\cdot\sigma_{\rm l}\cdot\tau_{\rm U}$, $I_{\rm ps}=h\nu_{\rm p}/(f_{{\rm L}i}+f_{{\rm U}j})\cdot\sigma_{\rm p}\cdot\tau_{\rm U}$)

$$\tau_{\rm U}\frac{{\rm d}X_{\rm U}(t,z)}{{\rm d}t}=I_{\rm p}(t,z)(f_{\rm p}-X_{\rm U}(t,z))-X_{\rm U}(t,z)-I_{\rm l}(t,z)(X_{\rm U}(t,z)-f_{\rm l}). \quad (6)$$

On the other hand, the absorption and the amplification processes will be described by the set of equations:

$$\frac{{\rm d}I_{\rm p}^{\varepsilon'}(t,z)}{I_{\rm p}^{\varepsilon'}(t,z)}=-\varepsilon'\alpha_0(t,z){\rm d}z,$$
$$\frac{{\rm d}I_{\rm l}^{\varepsilon}(t,z)}{I_{\rm l}^{\varepsilon}(t,z)}=\varepsilon g_0(t,z){\rm d}z, \quad (7)$$

where

$$\alpha_0=\sigma_{\rm p}N_{\rm Yb}(f_{{\rm L}i}+f_{{\rm U}j})(f_{\rm p}-X_{\rm U}),$$
$$g_0=\sigma_{\rm l}N_{\rm Yb}(f_{{\rm L}m}+f_{{\rm U}n})(X_{\rm U}-f_{\rm l}),$$

ε and ε' refer to the direction of propagation of the pump and the laser waves. Solving Eqs.(6) and (7), we get the stored energy and the extracted energy:

$$E_{\rm st0}=X_{U0}\cdot h\nu_{\rm p}=f_{\rm p}Y_{\rm p}\{1-\exp(-F_{\rm p}/Y_{\rm p})\}\cdot h\nu_{\rm p}, \quad (8)$$
$$E_{\rm ext}=(X_{U0}-X_{Ul})\cdot h\nu_{\rm l}=(X_{U0}-f_{\rm l}Y_{l0})\cdot\{1-\exp(-F_{l0}/Y_{l0})\}\cdot h\nu_{\rm l}, \quad (9)$$

where $Y_{\mathrm{p}0}$, $F_{\mathrm{p}0}$, $Y_{\mathrm{l}0}$, F_{l0} are the pump and laser fluence normalized to the pump saturation fluence and

$$Y_{\mathrm{p}0} = \frac{I_{\mathrm{p}0}}{1+I_{\mathrm{p}0}}, \quad F_{\mathrm{p}0} = I_{\mathrm{p}0}\frac{\tau_{\mathrm{p}}}{\tau_{\mathrm{U}}},$$

$$Y_{\mathrm{l}0} = \frac{I_{\mathrm{l}0}}{1+I_{\mathrm{l}0}}, \quad F_{\mathrm{l}0} = I_{\mathrm{l}0}\frac{\tau_{\mathrm{l}}}{\tau_{\mathrm{U}}}.$$

We now define two efficiencies of $\eta_{\mathrm{st}} = F_{\mathrm{st}}/F_{\mathrm{p}}$ and $\eta_{\mathrm{st-extr}} = F_{\mathrm{st-extr}}/F_{\mathrm{p}}$, where

$$F_{\mathrm{st}} = \int_0^L X_{\mathrm{U}} \times N_{\mathrm{Yb}} \times h\nu_{\mathrm{p}} \times \mathrm{d}l\,, \tag{10}$$

$$F_{\mathrm{st-extr}} = \int_0^L (X_{\mathrm{U}} - f_{\mathrm{l}}) \times N_{\mathrm{Yb}} \times h\nu_{\mathrm{p}} \times \mathrm{d}l\,, \tag{11}$$

where η_{st} and $\eta_{\mathrm{st-extr}}$ are the energy storage efficiency and extractable energy storage efficiency respectively. L is the thickness of the gain medium. F_{st}, $F_{\mathrm{st-extr}}$, and F_{p} are the stored pump fluence, extractable stored pump fluence and the total pump fluence respectively. Figure 2 shows that the extractable energy storage efficiency decreases significantly with increase of temperature since X_{U} is determined by f_{p}.

Figure 3 gives the longitudinal distribution of the temperature-related small-signal gain (SSG) coefficient within the disc which is pumped in single direction with a pump intensity of 15 kW/cm^2 and repetitive rate of 10 Hz. We can find that the average SSG coefficient decreases significantly from 2.4 to 1.3 cm^{-1} with increase of temperature in the lasing disc from 300 K to 350 K.

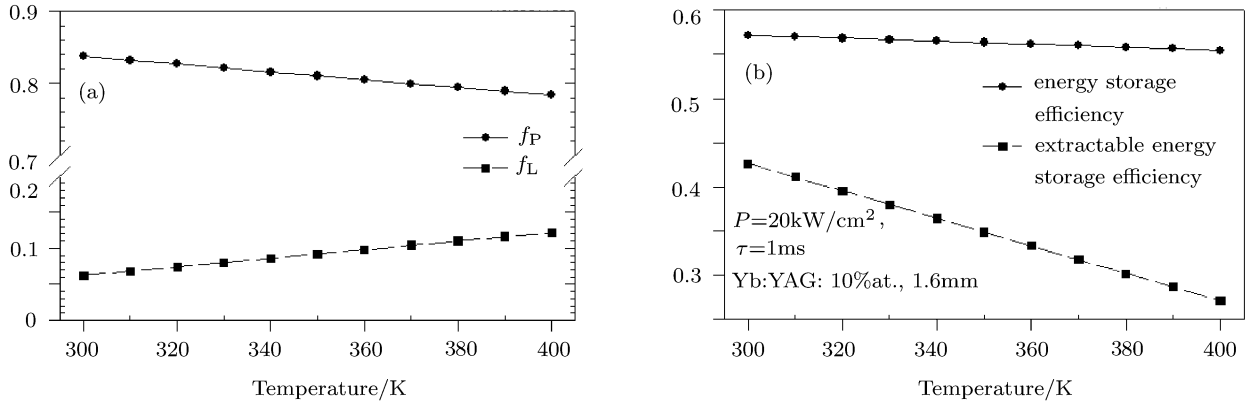


Fig.2. (a) Relationship between Boltzmann partition fraction and temperature, (b) Energy storage efficiencies $\mathrm{F_{st}/F}_P$ and $(\mathrm{F_{st}\text{-}F}_{extr})/\mathrm{F}_P$ versus temperature.

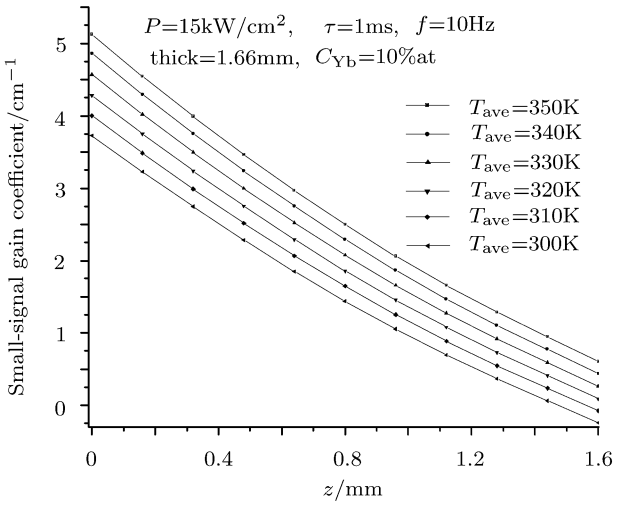


Fig.3. Longitudinal distribution of small-signal-gain coefficient within the disc for different temperatures.

3. Yb^{3+}: YAG diamond window cooled laser head design and numerical simulation

Cooling of a lasing disc along the axis of lasing is generally desirable, since the temperature gradient generated by the heat dissipation will be in the same direction as the axis of cooling. Consequently, the temperature will stay constant along the plane perpendicular to the cooling/lasing direction. In our diamond-cooled approach, the rear and front faces of gain disc is applied in good thermal contact to a thin plate of CVD diamond window; CVD diamond windows are transparent at the laser and pump wavelength and can be polished to optical quality so that they can be brought in close contact with the lasing disc. CVD thin diamond plates have exceptionally good thermal conduction properties. This property effectively causes the diamond plates to transfer the cooling effect of the peripherally applied water to the central areas of the plate, with minimal thermal resistance.[12]

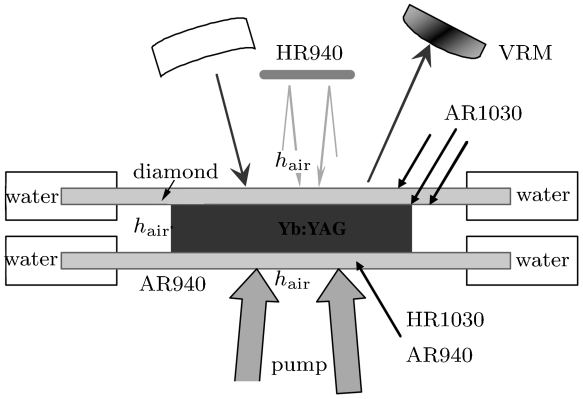


Fig.4. Schematic layout cross-sectional view of a diamond cooling laser head.

A schematic cross-sectional view of a diamond cooling Yb:YAG laser head is shown in Fig.4. The laser crystal is a disc-shaped 12mm×10mm× thickness (thickness will be optimized) Yb^{3+}:YAG, which has an antireflection coating at 1030 nm on 12mm×10mm surface. Yb^{3+} doping concentration will be optimized according to thickness of lasing disc. The pumping diode (at 940 nm) is composed of 40bars with a total emitting area of 33.2mm×26.0 mm and a maximum output power of 15 kW. The pump pulse duration is 1ms and the repetition rate is 10 Hz. The diamond window is cooled at its extremities in cooled water with heat exchange coefficient of h. Diamond surfaces are in air environment (free convection of air) with a coefficient of $h_{\rm air}$. The rear face of the diamond window (the one in pumping side of disc) is coated with antireflection coating at 940 nm and 1030 nm both to minimize pumping loss and lasing loss, while another diamond window is coated with antireflection coating at 1030 nm to minimize lasing loss. The pumping light is transmitted to the laser crystal via a lens duct, which is closely coupled to the diamond window, the transmission efficiency of the lens duct is about 81%. To increase the extraction efficiency of the stored energy on upper laser level, a V-shaped cavity is used.

3.1. Thermal power distribution in the lasing disc

According to the pumping absorption, we know that the pumping light absorption or thermal power deposition along x, y, and z directions are not uniform. Generally, $P_{\rm th}(y)$ has a very high order of super-Gaussian because of the use of lens duct (LD). $P_{\rm th}(x)$ is dependent on the alignment of each stack of LD and cylindrical lens which is used to collimate the LD output along the rapid axis. $P_{\rm th}(z)$ is also related to the doping concentration. A higher doping concentration will give rise to a more non-uniform distribution along thickness. However, a higher doping concentration corresponds to a thinner disc; as a result, thermal diffusion along the thickness will take less time. We can, however, make some reasonable assumptions to simplify the problem. First of all, because of the thermal diffusion is slow within medium ($\alpha = \kappa/\rho\, C_{\rm p} = 0.026$ cm^2/s), the characteristic thermal relaxation time along the thickness and radius are approximately 1.0 s and 14.0 s respectively. The interval between pump pulses is about 0.1 s for repetition of 10 Hz, so we can assume that the heat power source is continuous in time. Secondly, in the pumping area (about 7.6 mm×6.8 mm), thermal power is uniformly distributed along the medium surface. So, based on the physical model presented in section 2, the heat generation rate is calculated as follows:

$$P_{\rm th}(x,y,z) = I_{\rm abs}(x,y,z) \times \tau_{\rm P} \times F \times \eta_{\rm th}/l\,, \quad (12)$$

where $I_{\rm abs}$ is the absorption of pump intensity, $t_{\rm P}$ is the pump pulse duration, F is the repetition rate, $\eta_{\rm th}$ is the thermal efficiency, and l is the thickness of medium. Taking into account the quantum efficiency, we find that the Stokes loss of Yb^{3+}:YAG is of 8.6%

$(1-\lambda_p/\lambda_L)$, and the experimental results,[2] the thermal efficiency η_{th} is fixed at 11% in our calculations. Figure 5 gives the thermal power distributions along z direction of the gain medium for different values of the thickness and the doping concentration with a pump intensity of 15 kW/cm^2 and repetitive rate of 10 Hz.

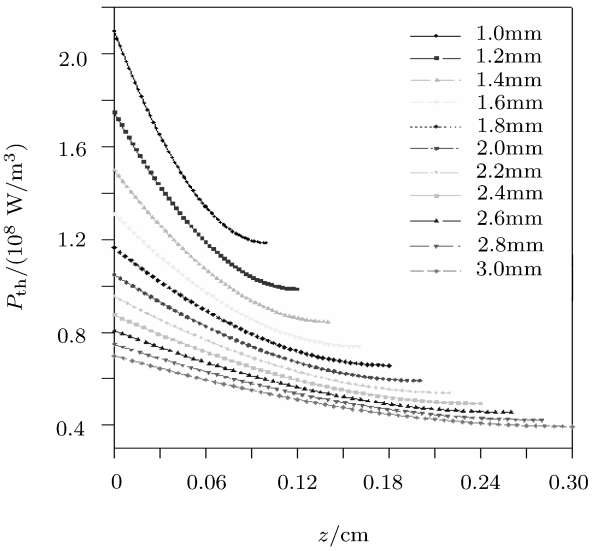


Fig.5. Thermal power distributions along the z direction.

3.2. Heat transfer equation and related parameters

The heat transfer equation is thus as follows:

$$\rho \cdot C_p \cdot \frac{\partial T(x,y,z;t)}{\partial t} = \kappa(T, C_{Yb}) \cdot \left(\frac{\partial^2 T}{\partial x^2} + \frac{\partial^2 T}{\partial y^2} + \frac{\partial^2 T}{\partial z^2}\right) + P_{th}(x,y,z), \quad (13)$$

where ρ is the mass density, C_p is the heat capacity, $P_{th}(x,y,z)$ is the heat generation rate within the gain medium introduced by pumping absorption, $\kappa(T, C_{Yb})$ is the temperature- and concentration-related thermal conductivity, On Fig.6, we plot the temperature- and concentration-dependent thermal conductivity of Yb^{3+}:YAG[13−15] based on the works of Gaumé *et al.*[8] Such a relationship will be used during the calculations.

$$\kappa(T,\, C_{Yb}) = C_1 * \exp(-C_5 * C_{Yb}^{C_7}) + C_2 * C_{Yb}^{C_6} + C_3 * C_{Yb} + C_4) * (300/T)\,, \quad (14)$$

where

$$C_1 = 5.3, \quad C_2 = -0.96, \quad C_3 = 0.018, \quad C_4 = 5.6, \quad C_5 = 0.18, \quad C_6 = 0.01, \text{ and } C_7 = 0.8.$$

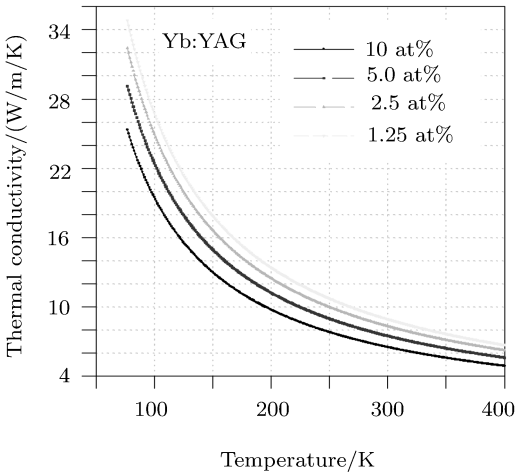


Fig.6. The relationship between thermal conductivity, temperature, and Yb concentration.

The other fixed parameters of lasing disc used in all calculations are: the mass density of 4.56×10^3 kg/m^3, the heat capacity of 0.59 $\times10^3$ J/kgK, The heat exchange coefficient of free convection of air (h_{air}) of 5 W/m^2 K, the temperature of 300 K for water and air. Parameters of CVD diamond used in calculations are: the dimension of 16mm×14mm×0.3 mm, the mass density of 3.515×10^3 kg/m^3, the heat capacity of 0.502×10^3 J/kgK, the thermal conductivity of 1800 W/m/K.

3.3. Numerical results and discussion

Because we do not know exactly the heat exchange coefficients of water (h), we calculate here the final steady state temperature distribution of the lasing disc at different values of h, which is usually between 1000–10000 W/m^2 K.[5]

From Fig.7 we can see that the overall cooling ability of the diamond plate is so effective that the maximum temperature in lasing disc has significantly decreased in comparison with the case that the plate is directly cooled by water. Figure 7 also shows that in our cooling scheme the heat exchange coefficient of water should be about 3000 W/m^2 K to keep the maximum temperature of the lasing disc below a reasonable value, e.g., less than 310 K.

Figure 8 shows that with increase of the heat exchange coefficient of water, the time necessary for dia-

mond window cooling to reach steady-state condition is decreased.

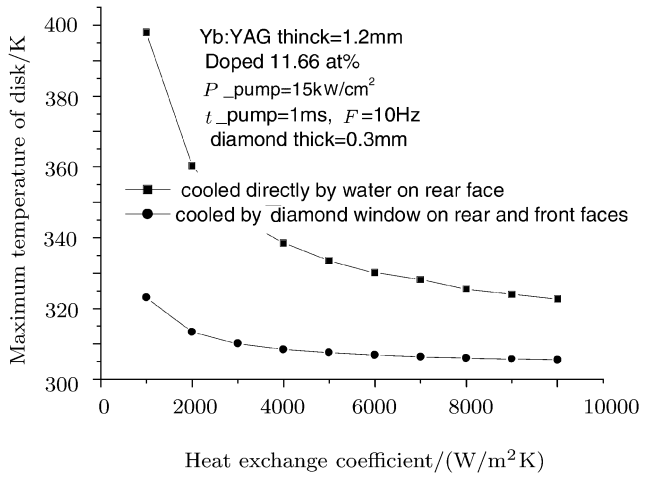


Fig.7. Lasing disc maximum temperature versus the heat exchange coefficients of water.

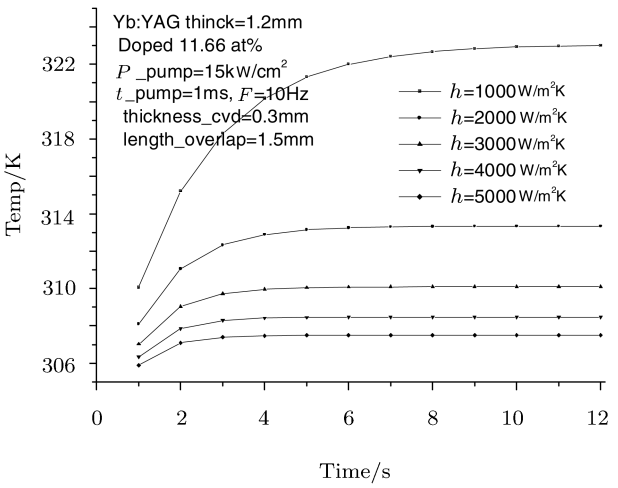


Fig.8. The temperature behaviour of the lasing disc.

The lasing disc centreline temperature along the x direction is shown in Fig.9. The temperature gradients perpendicular to beam is minor due to exceptionally good thermal conduction properties of diamonds. This effectively reduces the thermal lensing in the disc.

Although the total thermal energy is the same for each case, the average temperature for the thicker lasing disc is much higher since the thermal diffusion length is longer. The temperature difference along thickness is thus larger for the thicker lasing disc as shown in Fig.10

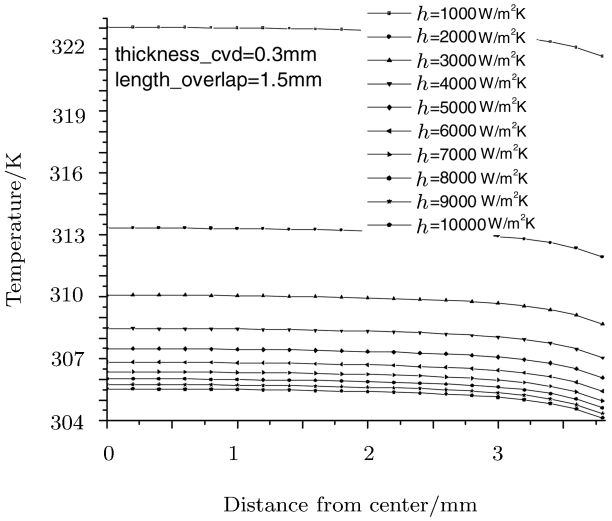


Fig.9. Temperature distribution of the lasing disc along the x direction centreline.

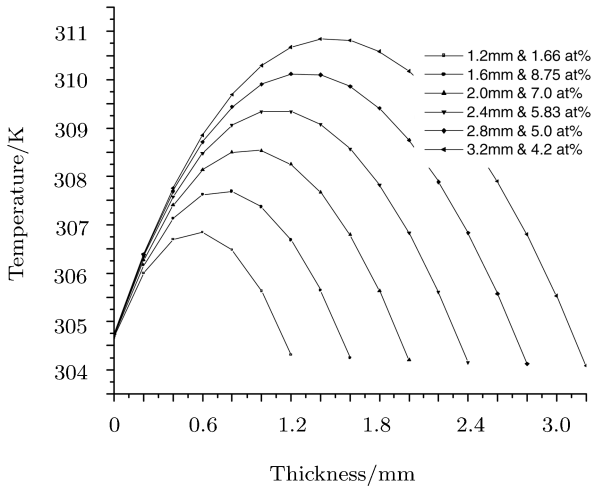


Fig.10. Temperature distribution of the lasing disc along the thickness direction centreline.

3.4. Optimization of the diamond dimensions

In this section we discuss the various considerations applied in choosing the diamond window dimensions. The diamond window must be wider than the crystal width in order to facilitate heat transfer to the cooling water at the circumference. The thickness should be as large as possible because the heat transfer capability of the window increases with thickness. But, the fact that the diamond window is an expensive

component (which increases linearly with its volume) dictates that an optimization should be performed.

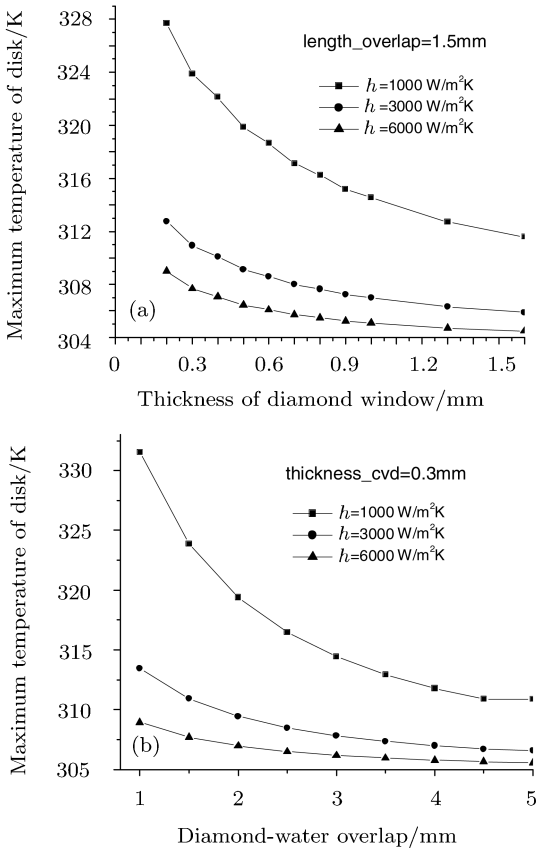


Fig.11. (a) Disc maximum temperature versus thickness of diamond windows. (b) Disc maximum temperature versus diamond-water overlap length.

Figure 11 shows the effect of varying the thickness of diamond and the overlap-length (overlap between the diamond and the water) on the maximum temperature of the crystal. Where the temperature of the cooling water is 300 K. One can see that increasing the thickness of the diamond and the overlap-length between diamond and water will decrease the maximum crystal temperature. From these simulations we conclude that a 0.3–0.5 mm thick diamond window with the overlap length of 2 mm will provide acceptable cost effective cooling.

4. Conclusions

The temperature-related performances of the Yb^{3+}:YAG disc laser has been investigated based on quasi-three level rate equation model. A novel cooling scheme using a diamond window whose heat conductivity is over 1800 W/m·K is also demonstrated. Based on these simulations we conclude that the 0.3–0.5 mm thick diamond window with the diamond–water overlap length of 2 mm will provide acceptable cost effective cooling, e.g., with a pump intensity of 15 kW/cm^2 and repetitive rate of 10Hz, to keep the maximum temperature of the lasing disc below a reasonable value (310 K), the heat exchange coefficient of water should be about 3000 W/m^{2}K.

References

[1] Hein J, Podleska S, Siebold M, Hellwing M, Bodefeld R, Sauerbey R, Ehrt D and Winizer W 2004 *Appl. Phys.* B **79** 419

[2] Fan T Y 1993 *IEEE J. Quantum Electron.* **6** 1457

[3] Wu H S, Yan P, Gong M L and Liu Qiang 2004 *Chin. Phys* **6** 871

[4] Bourdet G L 2000 *Appl. Opt.* **6** 966

[5] Haiwu YU and Bourdet G L 2005 *Appl. Opt.* **44** 6412

[6] Bourdet G L 2001 *Opt. Commun.* **200** 331

[7] Chen X B, Wang L, Lv L B, et al 2003 *Chin. Phys.* **11** 1246

[8] Xie G Q, Wang T, Zhu H Y and Qian L J 2006 *Chin. Phys.* **3** 14

[9] Gong C B, Chen C S, Song Q M and Zhu L 2004 *Chin. Phys.* **8** 1263

[10] Zhu H T, Lou Q H, Qi Y F *et al* 2005 *Acta Phys. Sin.* **12** 5648 (in Chinese)

[11] Bo Y, Gen A C, Bi Y, *et al* 2006 *Acta Phys. Sin.* **55** 1171 (in Chinese)

[12] Yitshak Tzuk, Alon Tal, Sharon Goldring, Yaakov Glick, Eyal Lebiush, Guy Kaufman and Raphael Lavi 2004 *IEEE J. Quantum Electron.* **3** 262

[13] Gaumé R, Viana B, Vivien D, Roger J P and Fournier D 2003 *Appl. Phys. Lett.* **7** 1355

[14] Patel F D, Honea E C, Speth J S, Payne A, Hutcheson R and Equall R 2001 *IEEE J. Quantum Electron.* **1** 135

[15] Dong J, Bass M, Mao Y, Deng P Z and Gan F X 2003 J. *Opt. Soc. Am.* B **9** 1975